Contribution from the Department of Chemistry, Tokyo Institute of Technology, O-okayama, Meguro-ku, Tokyo 152, Japan, and Division of Electronic Structure, Institute for Molecular Science, Myodaiji, Okazaki 444, Japan

Excited-State Lifetime of the Nonemissive Complex [(2,2′-4*H*-Bipyrazinium(1+))bis(2,2′-bipyridine)ruthenium(II)](3+)

Kazuteru Shinozaki,† Osamu Ohno,† Youkoh Kaizu,† Hiroshi Kobayashi,*,† Minoru Sumitani,‡ and Keitaro Yoshihara*,‡

Received November 28, 1988

$[Ru(bpz)(bpy)_2]^{2+}$ (bpz = 2,2′-bipyrazine; bpy = 2,2′-bipyridine) is protonated on the peripheral nitrogens of coordinated bipyrazine in acidic media. The protonated species $[Ru(bpzH)(bpy)_2]^{3+}$ emits no phosphorescence. By measurements of time-resolved absorption recovery of the ground-state species after saturated by pulse excitation, the excited-state lifetime of the nonemissive $[Ru(bpzH)(bpy)_2]^{3+}$ formed in acidic media was determined to be 1.1 ns, which is rather short in contrast with that of the deprotonated species $[Ru(bpz)(bpy)_2]^{2+}$ (88 ns). The nonradiative relaxation process in the protonated species is so accelerated that the protonation equilibrium of the excited species is not established in dilute acid solution during the short period of the excited-state lifetime. In dilute acidic media, $[Ru(bpz)(bpy)_2]^{2+}$ is recovered by proton dissociation following deactivation by diffusion-controlled proton attack of the excited complex. The present measurements determined the rate of proton dissociation ($k_{-2} = (1-2) \times 10^8$ s^{-1}) of the $[Ru(bpzH)(bpy)_2]^{3+}$ being formed by the nonradiative relaxation of the excited complex.

Introduction

The lowest excited state of $[Ru(bpz)(bpy)_2]^{2+}$ (bpz = 2,2′-bipyrazine) is the "metal-to-bipyrazine" charge-transfer excited triplet,[1] from which it emits intense phosphorescence in aqueous media even at room temperature. The excitation spectrum is in good agreement with the absorption spectrum, which exhibits a split metal-to-ligand charge-transfer absorption band (bands I and II). Resonance Raman modes of coordinated bipyrazine in $[Ru(bpz)(bpy)_2]^{2+}$ are observed as in $[Ru(bpz)_3]^{2+}$ upon irradiation at wavelengths within the lower energy component band (band I; ϵ_{max} = 488 nm) while those of coordinated bipyridine are detected as in $[Ru(bpy)_3]^{2+}$ upon irradiation in the higher energy component band (band II; ϵ_{max} = 406 nm).[2] The absorption spectrum varies with increasing $[H_3O^+]$, exhibiting isosbestic points, and shows the formation of the protonated species $[Ru(bpzH)(bpy)_2]^{3+}$ in acidified media. The protonated species emits no phosphorescence. Even in dilute acid solutions such that no protonated species can be detected in absorption spectrum, the phosphorescence of $[Ru(bpz)(bpy)_2]^{2+}$ is partly quenched by H_3O^+ in solution.[3]

Since the "metal-to-bipyrazine" charge-transfer excitation increases the basicity of the peripheral nitrogens of coordinated bipyrazine, the pK_a in the excited state (pK_a*) must be greater than the ground-state pK_a. In fact, a Förster cycle[4] predicts an increase in the excited-state basicity of coordinated bipyrazine.[3] However, if the nonradiative relaxation process of the protonated species is so accelerated that the protonation–deprotonation equilibrium cannot be established within the excited-state lifetime, the quenching in dilute acidic media is governed by the rate of diffusion-controlled encounter of H_3O^+ and the excited species. If it is the case, the ratio of emission yields in the absence and presence of H_3O^+, ϕ_0/ϕ, is given by

$$\phi_0/\phi = 1 + k_2^*\tau_0[H_3O^+] \quad (1)$$

where k_2* is the rate constant of diffusion-controlled protonation of the excited species and τ_0 is the excited-state lifetime. In such a situation, the observed displacement of the phosphorescence titration curve ϕ/ϕ_0 vs −log $[H_3O^+]$ from the curve obtained by the corresponding absorbance measurements should be ascribed to a difference of $1/(k_2^*\tau_0)$ and K_a but not to that of $(\tau_0'/\tau_0)K_a^*$ and K_a,[3] where τ_0' is the lifetime of $*[Ru(bpzH)(bpy)_2]^{3+}$.

The preceding paper concludes that the quenching process is governed by the diffusion-controlled protonation and the shift of titration curves obtained by absorption and emission intensity measurements is not a direct indication of the increase of excited-state basicity.[3] The conclusion, however, was inferred from the decay kinetics of $*[Ru(bpz)(bpy)_2]^{2+}$ in dilute acidic media without measurements of the decay rates of the nonemissive protonated excited species. In the present work, we determined the excited-state lifetime of the nonemissive protonated complex $*[Ru(bpzH)(bpy)_2]^{3+}$ by measurements of the time-resolved absorption recovery following saturation by pulse excitation. The lifetime of the protonated complex (1.1 ns) was much shorter than that of the deprotonated species (88 ns in H_2O). The present measurement supports the conclusion of the preceding paper.

Experimental Section

Preparation of the compound as well as the measurements of spectroscopy and luminescence decay lifetimes were described in the preceding paper.[3]

Determination of Excited-State Lifetimes of the Nonluminescent Complex. Lifetimes for ground-state repopulation of the excited complexes were measured by means of picosecond absorption spectroscopy.[5] Degassed solutions of 10^{-4} M in $[Ru(bpz)(bpy)_2]^{2+}$ with varied hydrogen ion concentrations (0–10.4 M) were excited by a single pulse shot of the third harmonic (354 nm; 15 ps full width at half-height) from a mode-locked Nd:YAG laser. Absorption intensity was measured by a high-speed channel plate photomultiplier (Hamamatsu Photonics R-1294U) using the monitoring wavelengths 480 and 550 nm selected through a Shimadzu-Bausch & Lomb monochromator from a Xe-flash source triggered by the excitation pulse. The time-resolved absorption recovery starting just after the pulse excitation was displayed on a 1-GHz oscilloscope (Tektronix 7104 equipped with a Model 7A29 amplifier) and recorded on a CCD video camera interfaced with an NEC PC9801-VM2 computer. Four runs were averaged. The recovery rates were determined by means of the least-squares method on an NEC PC9801-F2 computer. The time resolution in the present work was within 500 ps.

Results and Discussion

A bleaching of the 480-nm absorption maximum of $[Ru(bpz)(bpy)_2]^{2+}$ in aqueous solution was observed upon excitation by the third harmonic pulse from a Nd:YAG laser. The ground-state repopulation from the excited state gives rise to a recovery of the 480-nm band as shown in Figure 1. From the observed single exponential recovery, the lifetime of $[Ru(bpz)(bpy)_2]^{2+}$ was determined to be 89 ns, which was in good agreement with the lifetime determined by the single-photon-counting method (88 ns). This indicates no secondary reaction such as triplet–triplet annihilation is induced by the laser-pulse excitation.

† Tokyo Institute of Technology.
‡ Institute for Molecular Science.

(1) Rillema, D. P.; Allen, G.; Meyer, T. J.; Conrad, D. *Inorg. Chem.* **1983**, *22*, 1617.
(2) Shinozaki, K.; Matsuzawa, H.; Kaizu, Y.; Kobayashi, H. To be submitted for publication.
(3) Shinozaki, K.; Kaizu, Y.; Hirai, H.; Kobayashi, H. *Inorg. Chem.*, preceding paper in this issue.
(4) Förster, T. *Z. Elektrochem.* **1950**, *54*, 531. See also: Parker, C. A. *Photoluminescence of Solutions*; Elsevier: London, 1967; p 328.
(5) Nakashima, N.; Yoshihara, K. *J. Chem. Phys.* **1982**, *77*, 6040.

0020-1669/89/1328-3680$01.50/0

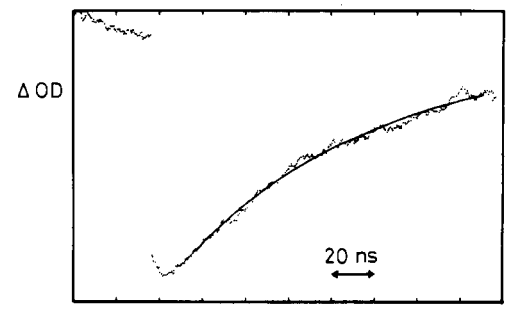

Figure 1. Recovery curve of the ground-state $[Ru(bpz)(bpy)_2]^{2+}$ in $[H_3O^+]$ = 0 M obtained by monitoring absorbance at 480 nm. The rate constant $k_1 = 1.1 \times 10^7\ s^{-1}$ (τ_0 = 89 ns) was obtained by the best fit (—).

Table I. Rates of Ground-State Absorbance Recovery and Phosphorescence Decay for a Variety of $[H_3O^+]$ in Aqueous Media

$[H_3O^+]$/M	monitoring wavelength[a]/nm	recovery rate/$10^8\ s^{-1}$	lifetime/ns	decay rate/$10^8\ s^{-1}$
0	480	0.11	88	0.11
0.02	480	1.2	3.7	2.7
0.2	480	2.4	0.7	14
1.2	480	3.7		
3.5	480	5.8		
	550	5.5		
5.8	550	8.8		
10.4	550	11		

[a] The recovery was measured by monitoring absorbance at 480 nm ($[Ru(bpz)(bpy)_2]^{2+}$) or at 550 nm ($[Ru(bpzH)(bpy)_2]^{3+}$).

The absorption spectrum of $[Ru(bpz)(bpy)_2]^{2+}$ varies with hydrogen ion concentration in aqueous media. $[Ru(bpzH)(bpy)_2]^{3+}$ exhibits a metal-to-bipyrazine charge-transfer (MLCT) band at 550 nm, while $[Ru(bpz)(bpy)_2]^{2+}$ shows the MLCT band at 480 nm.[1] The monoprotonated species $[Ru(bpzH)(bpy)_2]^{3+}$ is predominant at 6.0 M > $[H_3O^+]$ > 3.5 M, while the diprotonated species $[Ru(bpzH_2)(bpy)_2]^{4+}$ predominates at $[H_3O^+]$ > 8.0 M.[3] Both protonated species emit no phosphorescence.

In the present work, the recovery rates were measured with varied $[H_3O^+]$ in solution. The results are summarized in Table I. Regardless of the variety of $[H_3O^+]$, recoveries of the ground-state species are described by single exponentials. However, the recovery rate increases with increasing $[H_3O^+]$.

The recovery of $[Ru(bpzH)(bpy)_2]^{3+}$ was detected by measuring the time-resolved absorbance change at 550 nm in acidic solution $[H_3O^+]$ = 5.8 M, where $[Ru(bpzH)(bpy)_2]^{3+}$ is an exclusive species in solution. Figure 2 presents the observed recovery curve. The best fit of the recovery curve was obtained by use of the convolution method for the damped-oscillator profile of the excitation pulse. By application of the least-squares method, the recovery rate was determined to be $8.8 \times 10^8\ s^{-1}$. Thus the lifetime of the nonemissive complex $*[Ru(bpzH)(bpy)_2]^{3+}$ in acidic media is 1.1 ns. The recovery rate of $11 \times 10^8\ s^{-1}$ in $[H_3O^+]$ = 10.4 M indicates a reduction of the lifetime for further protonation ($*[Ru(bpzH_2)(bpy)_2]^{4+}$).

For a low hydrogen ion concentration such as $[H_3O^+] = 10^{-2}$–10^{-4} M where no protonated ground-state species is present in solution, phosphorescence of $[Ru(bpz)(bpy)_2]^{2+}$ is quenched by H_3O^+ in solution. The quenching rate constant was determined by lifetime measurements to be $k_q = 1.5 \times 10^{10}\ M^{-1}\ s^{-1}$. It is noted that the decay of $*[Ru(bpzH)(bpy)_2]^{3+}$, $k_1' = 8.8 \times 10^8\ s^{-1}$, is faster than the phosphorescence decay ($k_q[H_3O^+] = 1.5 \times 10^{10}[H_3O^+]\ s^{-1}$) in $[H_3O^+] = 10^{-2}$–10^{-4} M. This indicates the phosphorescence is quenched by diffusion-controlled encounter of H_3O^+ and $*[Ru(bpz)(bpy)_2]^{2+}$.

An identical straight line $1 + k_q\tau_0[H_3O^+]$ is obtained with Stern–Volmer plots of phosphorescence yields and lifetimes for a rather wide range of hydrogen ion concentration: $\phi_0/\phi = \tau_0/\tau = 1 + k_q\tau_0[H_3O^+]$. This is possible only when $k_1' \gg k_{-2}^*$ and thus the process turns out to be diffusion-controlled: $\phi_0/\phi = \tau_0/\tau = 1 + k_2^*\tau_0[H_3O^+]$.[3] In other words, the protonation equilibrium in the excited state is not established unless $k_1' \ll k_{-2}^*$.

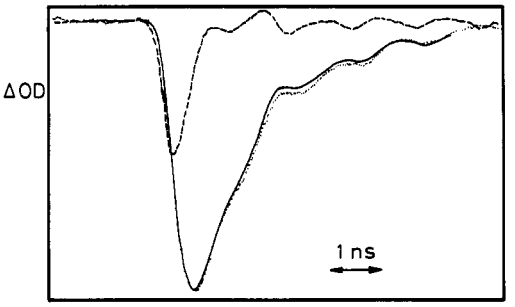

Figure 2. Recovery curve (···) of the ground-state $[Ru(bpzH)(bpy)_2]^{3+}$ in $[H_3O^+]$ = 5.8 M obtained by monitoring absorbance at 550 nm. The rate constant $k_1 = 8.8 \times 10^8\ s^{-1}$ (τ_0' = 1.1 ns) was determined by the best fit (—) obtained by use of the convolution method for the damped-oscillator profile of the excitation pulse (- - -).

In acidic media such as $[H_3O^+]$ = 0.2 and 0.02 M, a short-lived phosphorescence can be detected. If the protonation equilibrium of the excited species is fulfilled during the lifetimes of the excited species, the observed lifetime (τ) should continuously vary with increasing hydrogen ion concentration from τ_0 for $[H_3O]^+ = 0$ up to a plateau value τ_∞, and the excited-state proton-dissociation constant K_a^* ($=k_{-2}^*/k_2^*$) is given by [3]

$$K_a^* = \frac{k_1' - 1/\tau}{1/\tau - k_1}[H_3O^+] \qquad (2)$$

where k_1 ($=1/\tau_0 = 1.1 \times 10^7\ s^{-1}$) and k_1' ($=1/\tau_\infty = 8.8 \times 10^8\ s^{-1}$) are the intrinsic decay rates of $*[Ru(bpz)(bpy)_2]^{2+}$ and $*[Ru(bpzH)(bpy)_2]^{3+}$ and $1/\tau$ is the rate of phosphorescence decay observed as a function of $[H_3O^+]$. In $[H_3O^+]$ = 0.2 M, the decay rate ($1/\tau = 1.4 \times 10^9\ s^{-1}$) turns out to be greater than k_1'. Substitutions of these values ($1/\tau$, k_1, k_1') and $[H_3O^+]$ = 0.2 M into eq 2 yield a false equilibrium constant $K_a^* = -0.07$ M. This implies the protonation equilibrium is not established during the excited-state lifetime.

It is also noted that the recovery of $[Ru(bpz)(bpy)_2]^{2+}$ in dilute acidic media is slower than the phosphorescence decay. In dilute acidic media where the ground-state species is exclusively $[Ru(bpz)(bpy)_2]^{2+}$, phosphorescence is quenched by the encounter of H_3O^+ and $*[Ru(bpz)(bpy)_2]^{2+}$ in solution, while $[Ru(bpz)(bpy)_2]^{2+}$ is recovered by proton dissociation following the fast deactivation of $*[Ru(bpzH)(bpy)_2]^{3+}$ formed by collision of H_3O^+.

The concentrations of the excited species are given as a function of time delay t after the pulse excitation by

$$[*M] = [*M]_0 \exp(-\epsilon_1 t) \qquad (3)$$

$$[*MH^+] = \frac{k_2^*[H_3O^+]}{\epsilon_2 - \epsilon_1}[*M]_0 \exp(-\epsilon_1 t) + \left\{[*MH^+]_0 - \frac{k_2^*[H_3O^+]}{\epsilon_2 - \epsilon_1}[*M]_0\right\} \exp(-\epsilon_2 t) \qquad (4)$$

where $\epsilon_1 = k_1 + k_2^*[H_3O^+]$ and $\epsilon_2 = k_1'$ (see supplementary material for the derivation). The ground-state repopulation is detected by measuring absorbance at a wavelength λ as a function of the time delay:

$$\Delta[OD(\lambda,t)] = \epsilon(M,\lambda)\,([M] - [\overline{M}]) + \epsilon(MH^+,\lambda)\,([MH^+] - [\overline{MH^+}]) \qquad (5)$$

where $\epsilon(M,\lambda)$ and $\epsilon(MH^+,\lambda)$ are the molar absorbances of M and MH^+ at wavelength λ and $[\overline{M}]$ and $[\overline{MH^+}]$ are the corresponding equilibrium concentrations, respectively.

Since the 354-nm laser pulse gives rise to excitation at an isosbestic point of $[Ru(bpz)(bpy)_2]^{2+}$ and $[Ru(bpzH)(bpy)_2]^{3+}$, $[*M]_0$ and $[*MH^+]_0$ should be proportional to $[\overline{M}]$ and $[\overline{MH^+}]$. The values of k_1 ($=1.1 \times 10^7\ s^{-1}$) and k_1' ($=8.8 \times 10^8\ s^{-1}$) were determined by the recovery rates measured at $[H_3O^+]$ = 0 and 5.8 M, respectively. The value k_2^* can be determined by the quenching rate constant k_q measured with dilute acid solutions

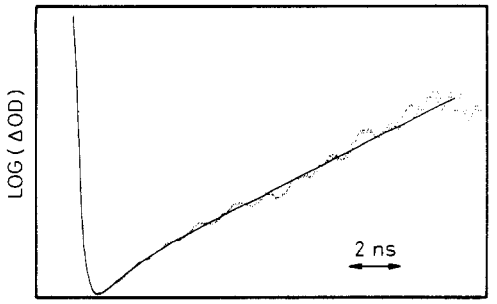

Figure 3. Observed (···) and calculated (—) recovery curves monitored at 480 nm for $[Ru(bpz)(bpy)_2]^{2+}$ in $[H_3O^+]$ = 1.2 M. By the best fit, the proton-dissociation and proton-association rate constants in the ground state were determined to be $k_{-2} = 1.8 \times 10^8$ s^{-1} and $k_2 = 1.7 \times 10^7$ M^{-1} s^{-1}, respectively.

Table II. Proton Dissociation (k_{-2}) and Association Constants (k_2, k_2^*) of $[Ru(bpz)(bpy)_2]^{2+}$

$[H_3O^+]$/M	monitoring wavelength[a]/nm	$[H_3O^+]/K_a$	$k_{-2}/10^8$ s^{-1}	$k_2/10^7$ M^{-1} s^{-1}	$k_2^*/10^{10}$ M^{-1} s^{-1}
0	480	0			
0.02	480	0.001	1.4	0.5	1
0.2	480	0.01	2.2	0.9	1
1.2	480	0.11	1.8	1.7	2
3.5	480	1.79	1.0	5.0	5
	550	1.79	1.1	5.7	5

[a] The recovery was measured by monitoring absorbance at 480 nm ($[Ru(bpz)(bpy)_2]^{2+}$) or at 550 nm ($[Ru(bpzH)(bpy)_2]^{3+}$).

($[H_3O^+] \ll K_a$; $[\overline{MH^+}]/[\overline{M}] = [H_3O^+]/K_a \sim 0$).

It should be noted that the rate constants k_2 and k_2^* vary with ionic strength in solution while k_{-2} is independent of ionic strength. In the present work, the ionic strength in solution was not adjusted to a constant value. The ionic strength certainly increases with increasing concentration of added acid. Since $1/K_a = k_2/k_{-2}$ can be determined by absorption measurements as a function of hydrogen ion concentration and k_{-2} and k_{-2}^* are independent of ionic strength, the observed recovery curves are simulated by optimization with respect to k_2 and k_2^*, both of which are assumed to have the same dependence on ionic strength as $1/K_a$. Figure 3 presents the observed and the calculated recovery curves in the case of $[H_3O^+]$ = 1.2 M. The proton-dissociation rate k_{-2} of $[Ru(bpzH)(bpy)_2]^{3+}$ in the ground state was evaluated to be 1.8×10^8 s^{-1}. Table II summarizes the evaluated rates of diffusion-controlled protonation of the excited species (k_2^*), and of proton dissociation and association (k_{-2}, k_2) of the ground-state species.

Concluding Remarks

The lifetime of a nonemissive protonated complex, $*[Ru(bpzH)(bpy)_2]^{3+}$, is as short as 1.1 ns in contrast with that of an emissive deprotonated complex, $*[Ru(bpz)(bpy)_2]^{2+}$ (88 ns). In dilute acidic aqueous media, where $[Ru(bpz)(bpy)_2]^{2+}$ is not protonated, the phosphorescence is quenched by a diffusion-controlled encounter of H_3O^+ and the excited complex. The fast nonradiative relaxation in the protonated species inhibits establishment of a protonation equilibrium of the excited complex during the excited-state lifetime.

Since both protonated and deprotonated species of $[Ru(bpy)_2(4,7\text{-dihydroxy-}1,10\text{-phenanthroline})]^{2+}$ are emissive in aqueous media and their lifetimes are not very different from each other, the proton-dissociation constants in the ground state and the excited state were determined by the spectral and lifetime measurements with varied $[H_3O^+]$.[6] The complex increases acidity in the excited state. On the other hand, excitation of $[Ru(bpy)_2(2,2'\text{-bipyridine-}4,4'\text{-dicarboxylic acid})]^{2+}$ results in a decrease in the acidity of the carboxylic groups attached to one of the coordinated bipyridines.[7] A displacement between the titration curves obtained by absorption and emission intensity measurements has been attributed to a shift of protonation equilibrium caused by electronic excitation.

In the case of $[Ru(bpz)(bpy)_2]^{2+}$, two different titration curves were also obtained with varied $[H_3O^+]$ by absorption and emission intensity measurements. The displacement, however, is due to the rate of diffusion-controlled protonation but is not a direct indication of the enhancement of excited-state basicity. In the present work, the rate constants of protonation for $*[Ru(bpz)(bpy)_2]^{2+}$ and $[Ru(bpz)(bpy)_2]^{2+}$ were determined to be $k_2^* \sim 2 \times 10^{10}$ M^{-1} s^{-1} and $k_2 = 1.7 \times 10^7$ M^{-1} s^{-1} (in $[H_3O^+]$ = 1.2 M), respectively. The protonation reaction occurs in two steps: migration of solvated proton toward the base followed by a proton attack on one of the peripheral nitrogens through the hydrogen-bonded complex. Most of the second-order rate constants for typical diffusion-controlled protonation are in the range from 10^{10} to 10^{11} M^{-1} s^{-1}.[8-10] On the other hand, the dissociation rate is rather slow (10^2–10^5 s^{-1}), indicating a large difference in the strength of the protonation bond broken. The N–H$^+$ bond in $[Ru(bpzH)(bpy)_2]^{3+}$ in the ground state is so weak that the deprotonation is rather fast ($k_{-2} = 1.8 \times 10^8$ s^{-1} in $[H_3O^+]$ = 1.2 M). In contrast with the low potential energy barrier in the deprotonation process, a high barrier is present in the protonation; the rate constant $k_2 = 1.7 \times 10^7$ M^{-1} s^{-1} is appreciably smaller than anticipated for the diffusion-controlled protonations. Thus, the rate constants of protonation of this particular complex in the ground state and the excited state are described by

$$k_2 = k_a \nu_2 \exp(-E_2/kT) \qquad k_2^* = k_a \nu_2^* \exp(-E_2^*/kT) \quad (6)$$

where E_2 and E_2^* are the activation energies of protonation in the ground state and the excited state, ν_2 and ν_2^* are the characteristic N···H$^+$–OH$_2$ stretching frequencies, and k_a is the diffusion-controlled bimolecular association rate, which is invariant regardless of whether the complex is in the ground state or in the excited state.[9] The protonation reaction is remarkably accelerated in the excited state ($k_2^* \sim 2 \times 10^{10}$ M^{-1} s^{-1}) up to nearly the limit of diffusion-controlled rate, $k_2^* \sim k_a$. Diffusing H_3O^+ may come to collision with the complex at various other sites than the peripheral nitrogens on the coordinated bipyrazine. However, an increase in k_2^* with reference to k_2 is ascribed to an reduction of the barrier in the activation-controlled process in protonation following the diffusion-controlled encounter. This is caused by an enhancement in ν_2^* and/or a reduction in E^*, both of which are induced by MLCT excitation of the complex. In fact, the Förster cycle calculation predicts K_a^* ($=k_{-2}^*/k_2^*$) is much decreased from the value of K_a = 1.4 M down to 6×10^{-9} M (in $[H_3O^+]$ = 3.0 M).[3] In the present work, the values $k_1' = 8.8 \times 10^8$ s^{-1} and $k_2^* \sim 2 \times 10^{10}$ M^{-1} s^{-1} were obtained, while the value of k_{-2}^* could not be experimentally determined; however, its order of magnitude can be estimated as $k_{-2}^* = K_a^* k_2^* \sim 1 \times 10^2$ s^{-1}. This implies that $k_1' \gg k_{-2}^*$. The Stern–Volmer constant $k_q = k_2^* k_1'/(k_1' + k_{-2}^*)$ is given by $k_q = k_2^*$ if $k_1' \gg k_{-2}^*$, while $k_q = (k_2^*/k_{-2}^*)/k_1'$ if $k_1' \ll k_{-2}^*$. The facts we observed in this work support the conclusion of the preceding paper that the quenching is to be a diffusion-controlled process. Therefore, the shift of the emission titration curve from the absorption titration curve is due to a difference of the equivalent points, $[H_3O^+] = 1/(k_2^* \tau_0)$ and K_a, but not that of $(\tau_0'/\tau_0)K_a^*$ and K_a. This conclusion, however, does not necessarily contradict the possibility of enhancement of the excited-state basicity predicted by the Förster cycle. In fact, it is concluded from the present observation that k_2^* greater than

(6) Giordano, P. J.; Bock, C. R.; Wrighton, M. S. *J. Am. Chem. Soc.* **1978**, *100*, 6960.
(7) Giordano, P. J.; Bock, C. R.; Wrighton, M. S.; Interrante, L. V.; Williams, R. F. X. *J. Am. Chem. Soc.* **1977**, *99*, 3187. Lay, P. A.; Sasse, W. H. F. *Inorg. Chem.* **1984**, *23*, 4123.
(8) Eigen, M. *Z. Elektrochem.* **1960**, *64*, 115; *Pure Appl. Chem.* **1963**, *6*, 97; *Angew. Chem.* **1963**, *75*, 489. Eigen, M.; De Maeyer, L. *Proc. R. Soc. London, A* **1958**, *247*, 505. *The Structure of Electrolyte Solutions*; Hamer, W. J., Ed.; Wiley: New York, 1959; p 64.
(9) Weller, A. *Z. Elektrochem.* **1960**, *114*, 55; *Prog. React. Kinet.* **1961**, *1*, 187.
(10) Amdur, I.; Hammes, G. G. *Chemical Kinetics Principles and Selected Topics*; McGraw-Hill: New York, 1966; p 148.

k_2 is attributable to a reduction of the barrier in protonation caused by an increase in the excited-state basicity.

Acknowledgment. This work was supported by the Joint Studies Program (1985-1986) of the Institute for Molecular Science. H.K. thanks Professor R. Watts, University of California, Santa Barbara, CA, for helpful comments.

Supplementary Material Available: Derivation of eq 3-5 (2 pages). Ordering information is given on any current masthead page.

Contribution from the Department of Chemistry, The University of Calgary, Calgary, Alberta T2N 1N4, Canada, and Laboratory of Solid State Chemistry and Mössbauer Spectroscopy and Laboratories for Inorganic Materials, Department of Chemistry, Concordia University, Montreal, Quebec H3G 1M8, Canada

Lewis Base Properties of 1,5-Diphosphadithiatetrazocines: Crystal and Molecular Structures of 1,5-$Ph_4P_2N_4S_2Me^+CF_3SO_3^-$

Tristram Chivers,*,† Georges Y. Dênès,‡ Stephen W. Liblong,† and John F. Richardson†

Received March 21, 1989

The behavior of 1,5-$Ph_4P_2N_4S_2$ (**2**; R = Ph) toward Lewis and Brønsted acids has been investigated, and the following adducts have been isolated: 1,5-$Ph_4P_2N_4S_2H^+BF_4^-$, 1,5-$Ph_4P_2N_4S_2Me^+CF_3SO_3^-$, 1,5-$Ph_4P_2N_4S_2{\cdot}BCl_3$, [1,5-$Ph_4P_2N_4S_2H_2^{2+}$][$CF_3SO_3^-$]$_2$ and (1,5-$Ph_4P_2N_4S_2$)$_4{\cdot}3SnCl_4$. The monoadducts show two equally intense doublets ($^4J_{PP}$ = 16-23 Hz) in the ^{31}P NMR spectra and exhibit a strong Raman band at 280-290 cm^{-1} attributed to an S-S stretching vibration. The structure of 1,5-$Ph_4P_2N_4S_2Me^+CF_3SO_3^-$ (**3**) has been determined by X-ray crystallography. The crystals of **3** are monoclinic, space group $P2_1/n$, with a = 14.231 (6) Å, b = 10.824 (3) Å, c = 19.326 (10) Å, β = 100.11 (4)°, V = 2930 (1) Å^3, Z = 4. The final R and R_w values were 0.075 and 0.078, respectively. The folded conformation of the $P_2N_4S_2$ ring is retained in **3**, and the cross-ring S-S interaction of 2.44 Å is significantly shorter than that of **2** (R = Ph) (d(S-S) = 2.53 Å). Coordination also causes a lengthening of the P-N and, especially, the S-N bonds involving the coordinated nitrogen to 1.67 and 1.68 Å from 1.62 and 1.60 Å, respectively, in **2** (R = Ph). The sum of the angles at the coordinated nitrogen atom is 358.0°. The ^{119}Sn Mössbauer spectrum of (1,5-$Ph_4P_2N_4S_2$)$_4{\cdot}3SnCl_4$ consists of a single line with δ = 0.73 mm s^{-1}, and the ^{31}P NMR spectrum of a solution of this complex shows a singlet at 111.6 ppm. A weakly coordinated structure involving three hexacoordinated tin atoms with trans-bridging 1,5-$Ph_4P_2N_4S_2$ ligands is proposed to account for these data. The ^{31}P NMR spectra of the diadducts 1,5-$Ph_4P_2N_4R_2^{2+}$ (R = H, Me) indicate the presence of symmetrically and asymmetrically substituted isomers that interconvert in solution.

Introduction

Recently we reported the interaction of the 1,3-diphosphadithiatetrazocine **1** (R = Ph) with Lewis and Brønsted acids.[1] It

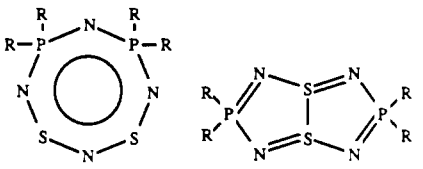

1 **2**

was observed that monoadduct formation occurs at a nitrogen between phosphorus and sulfur and, on the basis of an X-ray structural determinations of the methylated derivative, results in lengthening of the bonds (particularly from sulfur) to the coordinated nitrogen. The resulting polarization of π-electron density in the ring produces an -N=S=N- unit in the planar S_2N_3 moiety, which forms an angle of 108° with the PNP plane. The formation of symmetrical diadducts was also inferred on the basis of ^{31}P NMR data.

1,5-Diphosphadithiatetrazocines (**2**; R = Me, Ph), which are structural isomers of **1**, have been isolated and shown by X-ray crystallography to have folded structures with a weak cross-ring S-S interaction.[2,3] The low yields of the early syntheses of **2**, however, limited investigations of their reactivity to the oxidative addition of halogens, which occurs at the sulfur centers to give a trans-dihalogenated ring with loss of the S-S bond.[4] Recent improvements in the preparation of **2** (R = Me, Ph)[5] have facilitated further studies, and we describe here the Lewis base properties of **2** (R = Ph). No ambiguity exists over the site of coordination for monoadducts of **2**, since all four nitrogen atoms are chemically equivalent. However, the effect of adduct formation on ring conformation, particularly with regard to the loss or retention of the cross-ring S-S interaction, is of interest. The possible formation of diadducts, for which there are three structural isomers, is also worthy of attention.

The ring system **2** can be viewed as a hybrid of cyclotetraphosphazenes, $(R_2PN)_4$, and S_4N_4. For comparison, we note that the formation of monoprotonated derivatives of $(Me_2PN)_4$ gives rise to a minor perturbation of the ring conformation and an alternation of P-N bond lengths, the longest of which involve the coordinated nitrogen, that cannot be explained by inductive effects alone.[6] Diadducts of $(R_2PN)_4$ have also been structurally characterized.[6a,7] Monoadducts of S_4N_4, including the protonated derivative,[8] all form a flattened boat structure with loss of the cross-ring S-S interactions.

The crystalline adducts 1,5-$Ph_4P_2N_4S_2H^+BF_4^-$, 1,5-$Ph_4P_2N_4S_2Me^+CF_3SO_3^-$, 1,5-$Ph_4P_2N_4S_2{\cdot}BCl_3$, and (1,5-$Ph_4P_2N_4S_2$)$_4{\cdot}3SnCl_4$ have been isolated and characterized by ^{31}P NMR, Raman, and, in the case of the $SnCl_4$ adduct, ^{119}Sn Mössbauer spectroscopy. The structure of 1,5-$Ph_4P_2N_4S_2Me^+$-$CF_3SO_3^-$ was determined by X-ray crystallography. The formation of diadducts was monitored by ^{31}P NMR spectroscopy, and the

†The University of Calgary.
‡Concordia University.

(1) Chivers, T.; Liblong, S. W.; Richardson, J. F.; Ziegler, T. *Inorg. Chem.* **1988**, *27*, 4344.
(2) Burford, N.; Chivers, T.; Codding, P. W.; Oakley, R. T. *Inorg. Chem.* **1982**, *21*, 982.
(3) Burford, N.; Chivers, T.; Richardson, J. F. *Inorg. Chem.* **1983**, *22*, 1482.
(4) Burford, N.; Chivers, T.; Rao, M. N. S.; Richardson, J. F. *Inorg. Chem.* **1984**, *24*, 1946.
(5) Chivers, T.; Dhathathreyan, K. S.; Liblong, S. W.; Parks, T. *Inorg. Chem.* **1988**, *27*, 1305.
(6) (a) Trotter, J.; Whitlow, S. H.; Paddock, N. L. *J. Chem. Soc., Chem. Commun.* **1969**, 695. (b) Trotter, J.; Whitlow, S. H. *J. Chem. Soc. A* **1970**, 460.
(7) (a) Calhoun, H. P.; Oakley, R. T.; Paddock, N. L.; Trotter, J. *Can. J. Chem.* **1975**, *53*, 2413. (b) Trotter, J.; Whitlow, S. H. *J. Chem. Soc. A* **1970**, 455.
(8) Cordes, A. W.; Marcellus, C. G.; Noble, M. C.; Oakley, R. T.; Pennington, W. T. *J. Am. Chem. Soc.* **1983**, *105*, 6008.

0020-1669/89/1328-3683$01.50/0